Targeted Liposomal c-*myc* Antisense Oligodeoxynucleotides Induce Apoptosis and Inhibit Tumor Growth and Metastases in Human Melanoma Models

Fabio Pastorino,[1] Chiara Brignole,[1] Danilo Marimpietri, Gabriella Pagnan, Adriana Morando, Domenico Ribatti, Sean C. Semple, Claudio Gambini, Theresa M. Allen, and Mirco Ponzoni[2]

Differentiation Therapy Unit, Laboratory of Oncology [F. P., C. B., D. M., G. P., M. P.] and Laboratory of Pathology [A. M., C. G.], G. Gaslini Children's Hospital, 16148 Genoa, Italy; Department of Human Anatomy and Histology, University of Bari, Bari, Italy [D. R.]; Inex Pharmaceuticals, Burnaby, British Columbia, Canada [S. C. S.]; and Department of Pharmacology, University of Alberta, Edmonton, Canada [T. M. A.]

ABSTRACT

Purpose: **Melanoma is a highly malignant and increasingly common tumor. Because the cure rate of metastatic melanoma by conventional treatment is very low, new therapeutic approaches are needed. We previously reported that coated cationic liposomes (CCL) targeted with a monoclonal antibody against the disialoganglioside (GD_2) and containing c-*myb* antisense oligodeoxynucleotides (asODNs) resulted in a selective inhibition of the proliferation of GD_2-positive neuroblastoma cells *in vitro*.**

Experimental Design: **Here, we tested the *in vivo* antitumor effects of this novel antisense liposomal formulation by targeting the c-*myc* oncogene on melanoma, a neuroectodermal tumor sharing with neuroblastoma the expression of GD_2.**

Results: **Our methods produced GD_2-targeted liposomes that stably entrapped 90% of added c-*myc* asODNs. These liposomes showed a selective binding for GD_2-positive melanoma cells *in vitro*. Melanoma cell proliferation was inhibited to a greater extent by GD_2-targeted liposomes containing c-*myc* asODNs (aGD_2-CCL-myc-as) than by nontargeted liposomes or free asODNs. The pharmacokinetic results obtained after i.v. injection of [^{3}H]-myc-asODNs, free or encapsulated in nontargeted CCLs or GD_2-targeted CCLs, showed that free c-myc-asODNs were rapidly cleared, with less than 10% of the injected dose remaining in blood at 30 min after injection. c-myc-asODNs encapsulated within either CCL or aGD_2-CCL demonstrated a more favorable profile in blood, with about 20% of the injected dose of each preparation remaining *in vivo* at 24 h after injection. In an *in vivo* melanoma experimental metastatic model, aGD_2-CCL-myc-as, at a total dose of only 10 mg of asODN per kilogram, significantly inhibited the development of microscopic metastases in the lung compared with animals treated with myc-asODNs, free or entrapped in nontargeted liposomes, or aGD_2-CCL encapsulating scrambled asODNs ($P < 0.01$). Moreover, mice bearing established s.c. human melanoma xenografts treated with aGD_2-CCL-myc-as exhibited significantly reduced tumor growth and increased survival ($P < 0.01$ *versus* control mice). The mechanism for the antitumor effects appears to be down-regulation of the expression of the c-myc protein and interruption of c-*myc*-mediated signaling: induction of p53 and inhibition of Bcl-2 proteins, leading to extensive tumor cell apoptosis.**

Conclusion: **These results suggest that inhibition of c-*myc* proto-oncogene by GD_2-targeted antisense therapy could provide an effective approach for the treatment of melanoma in an adjuvant setting.**

INTRODUCTION

During the past decade, the worldwide incidence of melanoma has risen at a rate that equals or exceeds the majority of all other human solid malignancies (1, 2). Because metastatic or advanced-stage melanoma is refractory to conventional chemotherapy and/or radiation treatment, new therapeutic approaches are needed. The main limitation of current chemotherapeutic drug regimens in cancer therapy derives from the lack of specificity of the drugs, which can lead to severe systemic and organ toxicity. This impairs the use of high-dose intensity therapy, giving rise to a high rate of tumor relapse. The identification of fundamental genetic differences between malignant cells and normal cells resulting, for example, from activated oncogenes and inactivated tumor suppressor genes has made it possible to consider such genes as targets for antitumor therapy. The proto-oncogene c-*myc* belongs to a family of transcription regulators and is important for control of cell growth and differentiation (3). An association between changes in c-*myc* regulation and tumor formation has been reported (3). c-*myc* has also been found to induce apoptotic cell death under certain conditions (4, 5). Impaired apoptosis is a crucial step in tumorigenesis; indeed, neoplastic progression reflects loss of normal apoptotic mechanisms (4–6). Moreover, impaired apoptosis is also a significant impediment to cytotoxic therapy (6), and more rational therapy should emerge from clarifying how particular agents elicit ap-

Received 4/8/03; revised 5/29/03; accepted 5/30/03.
The costs of publication of this article were defrayed in part by the payment of page charges. This article must therefore be hereby marked *advertisement* in accordance with 18 U.S.C. Section 1734 solely to indicate this fact.
This work was supported by Fondazione Italiana per la lotta al Neuroblastoma, the Associazione Italiana Ricerca Cancro, and the National Cancer Institute of Canada. F. P. is a recipient of a Fondazione Italiana per la lotta al Neuroblastoma fellowship.
[1] These authors contributed equally to this work.
[2] To whom requests for reprints should be addressed, at Differentiation Therapy Unit, Laboratory of Oncology, G. Gaslini Children's Hospital, Largo G. Gaslini 5, 16148 Genoa, Italy. Phone: 39-010-5636342; Fax: 39-010-3779820; E-mail: mircoponzoni@ospedale-gaslini.ge.it.

optosis. Despite intensive research, the molecular mechanisms underlying c-*myc*-mediated apoptosis are yet to be completely understood. p53-Dependent and -independent mechanisms have been reported, and c-*myc*-induced apoptosis can be prevented by overexpression of the Bcl-2 oncoprotein (6, 7).

asODNs[3] are a new class of antineoplastic agents that can prevent the initiation or progression of specific human cancers when targeted to appropriate molecular targets (8, 9). In recent years, asODNs have shown efficacy in the selective inhibition of gene expression (9–12). asODNs that target c-*myc* have been shown to be therapeutically useful either alone or in combination with other drugs (13–15). However, the low physiological stability, unfavorable pharmacokinetics, low cellular uptake, and lack of tissue specificity limit therapeutic applications of asODNs (16). The use of lipid-based delivery systems represents an alternative to chemical modifications (17, 18) for increasing the stability of asODNs in blood circulation and for improving their disease-site delivery and cell permeability. It has been reported that liposomal asODN formulations of *raf* enhance the plasma and tissue levels of asODNs and improve its antitumor effects (19). Liposomes are also able to facilitate the delivery of antisense targeting the *Bcl-2*, *MDR1*, and c-*myc* genes *in vivo* (20–22). Sterically stabilized immunoliposomes, which have cell surface-directed antibodies grafted on their exteriors, have been recognized as efficient tools for the selective delivery of drugs and diagnostic agents to target cells (23).

Among the antigens found on malignant cells, GD_2 is an attractive target for immunoliposomal therapy of tumors of neuroectodermal origin (24–26), because it has high levels of expression in these tumors (27) but is less common in nonmalignant tissues. Recently, we demonstrated that c-*myb* asODNs entrapped in this novel GD_2-targeted liposomal formulation inhibited neuroblastoma growth *in vitro*, by specifically reducing c-myb protein expression (28). Here, we investigated whether sterically stabilized, GD_2-targeted liposomes containing aGD_2-CCL-myc-as can selectively deliver to melanoma cells sufficient amount of asODNs to effectively reduce c-myc protein expression and to inhibit *in vivo* tumor growth.

MATERIALS AND METHODS

Chemicals and mAbs. Hydrogenated soy phosphatidylcholine, cholesterol, DSPE-PEG, 1,2-dioleoyl-3-trimethylammonium propane, and rhodamine phosphatidylethanolamine were from Avanti Polar Lipids, Inc. (Alabaster, AL). A derivative of DSPE-PEG, with a maleimide group at the distal terminus of the polyethylene glycol chain (DSPE-PEG-maleimide), was synthesized by Shearwater Polymers (Huntsville, AL). [^{3}H]cholesteryl hexadecyl ether was from DuPont New England Nuclear (Boston, MA). All of the other reagents of biochemical and molecular biology grade were obtained from Sigma Chemical Co. (St. Louis, MO).

ODNs. The 16-mer phosphorothioate ODN against c-*myc* was provided by Inex Pharmaceuticals (Burnaby, British Columbia, Canada). Purity was >95% by high-performance liquid chromatography analysis. The asODN, referred to hereafter as myc-as, is complementary to the translation region of human c-*myc* mRNA and has the sequence 5′-TAACGTT-GAGGGGCAT-3′ (INX-6295). A scrambled sequence (INX-6300) containing the G-quartet motif (5′-TAAGCAT-ACGGGGTGT-3′) ODN was used as control (myc-scr). [^{3}H] INX-6295 was synthesized and purified by TriLink BioTechnologies (San Diego, CA) with a [^{3}H] thymidine base incorporated during synthesis at the position underlined above.

Liposome Preparation, ODN Encapsulation, and Coupling of Anti-GD_2 mAbs. c-myc-asODN was entrapped in liposomes using the CCL procedure of Stuart *et al.* (21, 29), slightly modified by us (28).

A recently described method (30), slightly modified by us (24, 28), was used to covalently link mAbs to the maleimide terminus of DSPE-PEG-maleimide. Briefly, we used 2-iminothiolane (Traut's reagent) to convert exposed amino groups on the antibody into free sulfhydryl groups. After separation of thiolated mAb from iminothiolane, the mAb was slowly added to a 5-ml test tube containing the liposomes (with encapsulated ODNs) and a small magnetic stirring bar. Optimal coupling was obtained using a PL:mAb mole ratio of 1500:1. Running a slow stream of nitrogen over the reaction mixture displaced oxygen. The tube was capped and sealed with Teflon tape, and the reaction was incubated overnight at room temperature with continuous slow stirring. The resulting immunoliposomes were separated from unreacted mAb by chromatography using Sepharose CL-4B and were sterilized by filtration through 0.2-μm pore cellulose membranes (Millipore Corp., Bedford, MA) and stored at 4°C. Coupling of mAbs to liposomes was quantified by adding trace amounts of ^{125}I-labeled mAb to the liposomes, followed by gamma counting (Cobra 5002; Canberra Packard, Meriden, CT).

Cell Lines and Culture Conditions. To broadly cover the phenotypes exhibited by melanoma cells *in vitro*, we used four GD_2-positive melanoma cell lines: NG, MZ2-MEL, COLO 853, and RPMI 7932 (24). Two GD_2-negative adherent cell lines, A-431 (human epidermoid carcinoma) and HeLa (human cervical carcinoma), were used in some experiments. All cell lines were maintained in the logarithmic phase of growth at 37°C in 75-cm^2 plastic culture flasks (Corning Inc., Corning, NY) in a 5% CO_2-95% air humidified incubator, split, washed, counted, and replated in fresh complete medium (RPMI 1640; Biochrom, Berlin, Germany), as described previously (24, 31). A 1 mM EDTA solution in HBSS (Flow Laboratories, Milan, Italy) was used to release adherent cell lines from the surface of the culture flasks.

Cellular Association Studies. The cellular association with melanoma cells of immunoliposomes targeted via aGD_2 was analyzed by flow cytometry (FACS). Liposomes were prepared as described previously with the addition of rhodamine

[3] The abbreviations used are: ODN, oligodeoxynucleotide; asODN, antisense ODN; myc-as, c-myc-asODN; mAb, monoclonal antibody; GD_2, disialoganglioside; CCL, coated cationic liposomes; aGD_2-CCL, GD_2-targeted CCL; CCL-myc-as, myc-asODNs encapsulated in nontargeted CCL; aGD_2-CCL-myc-as, myc-asODNs encapsulated in GD_2-targeted CCL; aGD_2-CCL-myc scr, scrambled myc-ODNs encapsulated in GD_2-targeted CCL; PL, phospholipid; DSPE-PEG, 1,2-distearoylglycero-3-phosphatidylethanolamine-*N*-polyethylene glycol-2000; FACS,fluorescence-activated cell sorting; IHC, immunohistochemistry; TUNEL, terminal deoxynucleotidyltransferase-mediated nick end labeling; CI, confidence interval.

phosphatidylethanolamine at 1 mol % of total PL, as described (24). Aliquots of cells (1×10^6/tube) were incubated for 1 h at 4°C with nontargeted (CCL-myc-as) or targeted (aGD_2-CCL-myc-as) liposomes. The cells were subsequently washed with PBS and were enumerated by flow cytometry. All of the cytometry experiments were performed using a FACScan instrument for FACS (Becton-Dickinson Immunocytometry Systems).

***In Vitro* Inhibition of Cell Growth.** MZ2-MEL, NG, or A-431 cells were plated in T-25 culture flasks (Corning) and treated with free myc-as, CCL-myc-as, aGD_2-CCL-myc-as, or with control ODN sequences encapsulated in targeted liposomes (aGD_2-CCL-myc-scr). One hundred micrograms per milliliter of the various ODN formulations were added to cells at the beginning of the experiment and every other day thereafter. Two hours after each addition, the cells were washed to remove unbound ODNs and transferred to fresh complete medium. All experiments were continued for 8 days; at 2-day intervals thereafter, the cells were detached with EDTA, stained with trypan blue, and counted microscopically.

Pharmacokinetic Experiments. Outbreed female BALB/c mice, 6–8 weeks of age, were purchased from the Health Sciences Laboratory Animal Services, University of Alberta. BALB/c mice (20–30 g) received injections via the tail vein (i.v.) of a single dose of free or liposomal asODNs, with or without coupled aGD_2, in a total volume of 0.2 ml (0.5 μmol PL/mouse). Radioactive counts (^{3}H-asODNs) for each injection ranged from 1 to 4×10^5 cpm. At selected time points (0.5, 2, 6, and 24 h) after injection, mice (three mice/group) were anesthetized with halothane and euthanized by cervical dislocation. A blood sample (100 μl) was collected by heart puncture and counted for the [^{3}H] label in a Beckman LS-6800 Scintillation beta counter. Blood correction factors were applied to all samples (21). In these experiments and the experiments below, all procedures involving animals and their care were in accordance with institutional guidelines and in compliance with national and international laws and policies.

Determination of Antitumor Activity *in Vivo*. Female athymic nude (nu/nu) mice, 4–6 weeks of age, were purchased from Harlan Laboratories (Harlan Italy, S.Pietro al Natisone, Italy) and kept under specific pathogen-free conditions.

For the lung metastasis experimental model, female nude mice (10 mice/group) received injections of MZ2-MEL cells (5×10^6 cells in 200 μl of HEPES-buffered saline) i.v. in the tail vein. By this route, cellular implantation resulted in a homogeneous, but slow, tumor growth, with 100% tumor take in the lung after 5 months. However, experimental lung metastases were already observed in about 3 months in 70–90% of mice. Animals were treated i.v. on days 1, 8, 15, and 22 after inoculation of cells at a dose of 2.5 mg of asODN per kilogram. For each experiment, mice received one of the following treatments: HEPES-buffered saline, free-myc-as, CCL-myc-as, aGD_2-CCL-myc-as, or aGD_2-CCL-myc-scr. Mice were monitored routinely for weight loss. Histological evaluation of microscopic metastases was performed for all tissues. Organs were fixed in neutral buffered 10% formalin, processed by standard methods, embedded in paraffin, sectioned at 5 μm, and stained with H&E for IHC.

For the s.c. tumor model, 5×10^6 MZ2-MEL cells were injected s.c. in the mid-dorsal region of mice. Tumors were allowed to grow for 5 days, and then i.v. asODN treatment (with the same formulations as above) was initiated with 3.5 mg of asODN per kilogram every day for 3 days. Tumor were measured twice weekly with calipers, and tumor volumes were calculated by the formula $\pi/6\ [w_1 \times (w_2)^2\ ]$, where w_1 represented the largest tumor diameter and w_2 represented the smallest tumor diameter. The body weight and general physical status of the animals were recorded daily, and the mice were terminated when the tumor reached 2000 mm^3.

Western Blot Analysis in Melanoma Tumor Xenografts. At 24-h intervals after terminating treatment of the s.c. tumors, mice were sacrificed by cervical dislocation, and their tumors were removed, immersed in HBSS, homogenized with the use of a Polytron PT 3000 (Kinematica AG, Littau, Switzerland), and solubilized in lysis buffer, as described previously (28, 31). Each tumor lysate was obtained from a pool of three different tumors grown in mice treated with the different formulations. Briefly, 30-μg samples of protein were subjected to 10% SDS-PAGE, with prestained molecular weight markers run in parallel to identify c-myc (M_r 64,000 to M_r 67,000), p53 (M_r 53,000), and Bcl-2 (M_r 26,000) proteins. The resolved proteins were blotted onto nitrocellulose membranes, and the mAbs anti-c-myc, anti-p53 (clone 9E10 and Pab 240, respectively; Santa Cruz Biotechnology, Santa Cruz Biotechnology, CA), and anti-Bcl-2 (clone 124; DAKO A/S, Glostrup, Denmark) were used to localize the corresponding polypeptides on the blots. Peroxidase-conjugated goat antimouse antibody was used as a secondary antibody. Immune complexes were visualized with the use of an enhanced chemiluminescence system (Amersham International, Little Chalfont, Buckinghamshire, United Kingdom) according to the manufacturer's instructions.

To determine whether approximately equal amounts of protein were loaded in samples, the stripped nitrocellulose membranes were stained with a mAb antihuman β-actin (clone C4; Boehringer Mannheim Inc., Mannheim, Germany). Levels of c-myc, p53, and Bcl-2 were quantified by scanning densitometry of the autoradiography films and normalized to β-actin levels.

Histological Analysis and Detection of Apoptosis in Tumor Xenografts. Paraffin-embedded tissue sections (5 μm) were examined after staining with Mayer's H&E (Sigma Chemical Co.). Staining for melanoma cells and cell proliferation were performed using the mAbs antihuman melanoma S-100 (clone 15E2E2) and the Ki67 antigen (clone Ki88 MIB-1), respectively (BioGenex, San Ramon, CA). p53 and Bcl-2 staining was performed using mAbs antihuman p53 and Bcl-2, respectively (clones DO-7 and 124; DAKO), and CD31 staining was performed by the use of an antimouse mAb (CD31; DAKO), as described previously (32). TUNEL staining was performed using a commercially available apoptosis detection kit (In Situ Cell Death Detection, horse radish peroxidase; Roche Molecular Biochemicals, Mannheim, Germany) according to the manufacturer's instructions.

Statistical Methods. Results are expressed as means ± 95% CIs. All *in vitro* data derive from at least three independent experiments. All of the *in vivo* experiments have been performed at least twice with similar results. Incidence of lung metastasis between groups was compared using Fisher's exact test. Peto's log-rank test determined the significance of the differences between experimental groups in the survival exper-

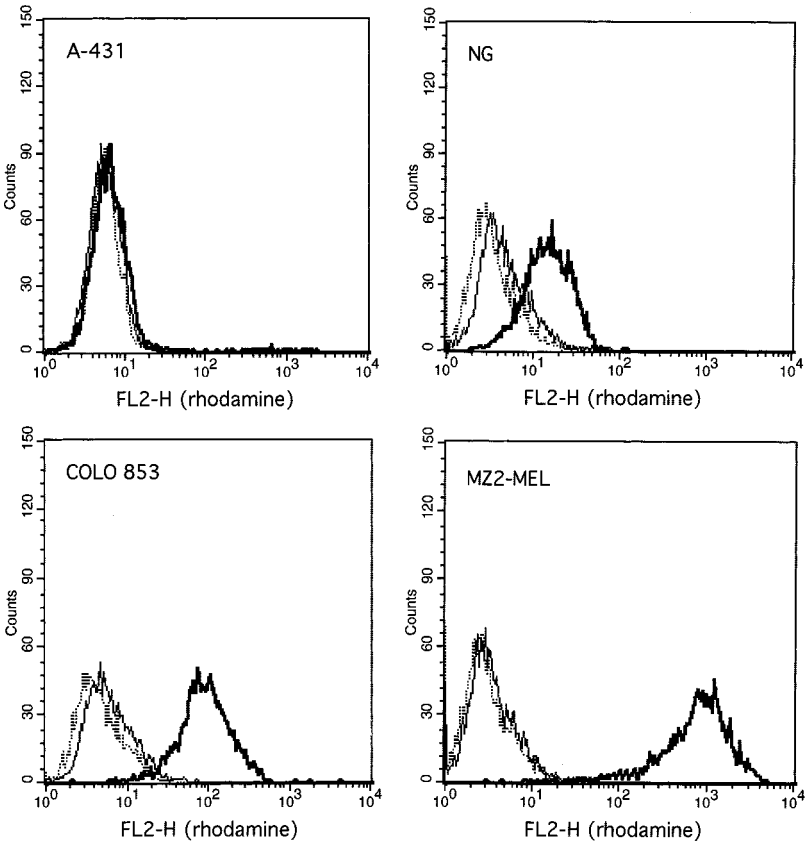

Fig. 1 Cellular association of immunoliposomes with GD_2-positive (NG, MZ2-MEL, and COLO 853) and GD_2-negative (A-431) tumor cells by flow cytometry. Cells were incubated for 1 h at 4°C with 600 nmol of PL per milliliter of rhodamine-labeled liposomes with encapsulated c-myc-asODNs with (*bold line*) or without (*thin line*) coupled anti-GD_2 mAbs. *Dotted line*, control cells.

iments by the use of StatsDirect statistical software (CamCode, Ashwell, United Kingdom).

RESULTS

Characterization of GD_2-targeted Immunoliposomes and Binding to Melanoma Cells. Liposomes prepared by our procedure are typically 110–130 nm in diameter, with an average coupling efficiency for the anti-GD_2 antibody of 65% (95% CI, 50–80%), resulting in an antibody density of 40–60 μg mAb/μmol PL. The efficiency of asODN entrapping in liposomes was approximately 90%, and during 4 h of dialysis at 37°C in 25% human plasma, 10–20% of asODNs were released and continued dialysis for up to 1 week produced no more free asODN. Finally, our dialyzed liposomes retained their ability to bind to GD_2-expressing cells over these same time periods, concordant with our previous results (28).

We studied the levels of cellular association of aGD_2-targeted or nontargeted liposomes to four GD_2-positive human melanoma cell lines [NG, MZ2-MEL, COLO 853 (Fig. 1), and RPMI 7932 (data not shown)] and two GD_2-negative cell lines, A-431 (Fig. 1) and HeLa (data not shown). The data showed that the level of cellular binding of liposomes is dependent on GD_2 expression in the different cell lines. aGD_2-CCL-myc-as showed a much higher cellular association to all of the GD_2-positive cell lines, compared with CCL-myc-as. In contrast, the GD_2-negative cell line A-431 showed very low, if any, levels of liposomes associated with the cells for both targeted and nontargeted formulations (Fig. 1).

Effect of Immunoliposome-Encapsulated c-*myc* asODNs on Melanoma Cell Proliferation *in Vitro*. To assess the efficiency of GD_2-targeted liposomes in delivering myc-as to target cells and to determine the effects of myc-as on melanoma cell proliferation, we used a protocol that allows high levels of antibody-mediated binding while minimizing nonspecific adsorption of liposomes to cells (24, 28). In these experiments, tumor cells were exposed to ODNs for 2 h at the beginning of the experiment and every 2 h every other day thereafter for a total of 8 days and then washed and transferred to ODN-free complete medium. Under these conditions, aGD_2-CCL-myc-as induced a marked decrease in melanoma cell proliferation (Fig. 2). In contrast, free myc-as and CCL-myc-as had significantly less cytotoxic effect on NG and MZ2-MEL cells. Under the same conditions, none of our ODN formulations inhibited proliferation of the GD_2-negative cell line A-431. To demonstrate the sequence specificity of these effects, scrambled-sequence ODNs were also delivered into NG, MZ2-MEL, and A-431 cells. Little or no growth inhibition was observed for aGD_2-CCL-myc-scr (Fig. 2).

Plasma Pharmacokinetics of Immunoliposome-Encapsulated c-*myc* asODNs in Mice. Fig. 3 shows the clearance from blood of both free and liposomal [^{3}H]-labeled asODNs injected into the tail vein of BALB/c mice. The results are

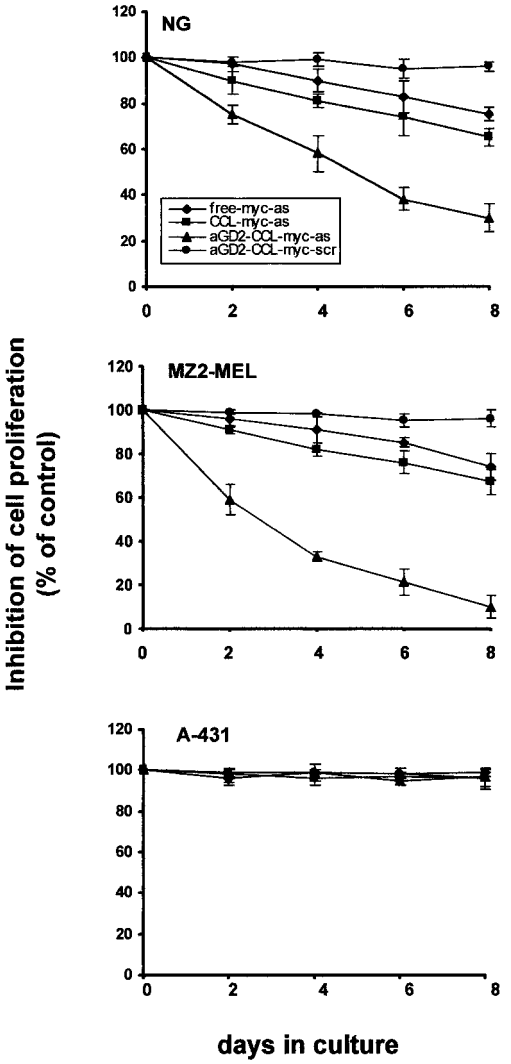

Fig. 2 Growth inhibition *in vitro* of melanoma cells by c-myc-asODNs encapsulated in anti-GD_2 liposomes. Cells were treated with 100 μg/ml free c-myc-asODNs (free-myc-as), asODNs encapsulated in liposomes without (CCL-myc-as) or with (aGD_2-CCL-myc-as) anti-GD_2 mAbs and scrambled sequence encapsulated in GD_2-targeted liposomes (aGD_2-CCL-myc-scr), as described in "Materials and Methods." Data are expressed as percentage of control, and the *bars* are 95% CIs.

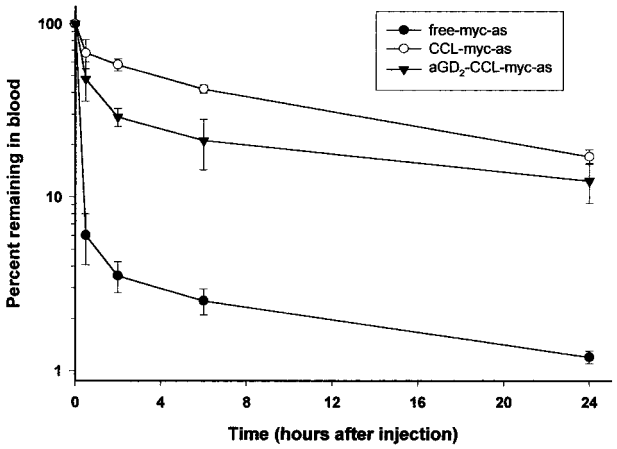

Fig. 3 Blood clearance kinetics of [^{3}H]-labeled c-myc-asODNs after i.v. injection into BALB/c mice. [^{3}H]-c-myc-asODNs were injected either free (free-myc-as, ●) or encapsulated in nontargeted (CCL-myc-as, ○) or targeted (aGD_2-CCL-myc-as, ▼) liposomes. At different times after injection, blood was collected and counted for the [^{3}H] label. Each point represents the average of three mice ± CI.

expressed as the percentage of the administered dose remaining in blood (33). When [^{3}H]-labeled asODN (from scintillation counting) and intact asODN (by dot blot) were compared previously, the [^{3}H] asODN proved to be an excellent marker for intact asODN (22, 29).

Free asODN was rapidly cleared, so that less than 10% of the injected dose remained in blood 30 min after injection. At this time point, approximately 40% of the injected dose had already been eliminated from the body, possibly through the kidneys, whereas most of the remaining radioactive counts resided in the carcass, liver, and kidneys (Ref. 21 and data not shown). At 24 h after injection, approximately 1% of the injected dose remained in blood. [^{3}H]-labeled asODN encapsulated within CCL demonstrate a much different blood profile. CCL had an initial phase of rapid clearance, which accounted for only around 30% of the injected dose. The remainder was cleared with a $T_{1/2}$ of approximately 4 h. At 24 h after injection, approximately 20% of the injected dose remained in blood. [^{3}H]-labeled asODN entrapped within aGD_2-CCL displayed a similar profile to CCL, however, the initial clearance phase accounted for approximately 50% of the injected dose. The remaining dose had clearance kinetics similar to the nontargeted asODN formulation, and 24 h after injection, over 10% of the injected dose remained in the blood.

Inhibition of Growth and Metastasis of Human Melanoma in Nude Mice by Immunoliposome-Encapsulated c-myc-asODNs. On the basis of the *in vitro* studies, we postulated that inhibition of c-*myc* functions in human melanomas might significantly impair or block their tumor-forming capabilities *in vivo*.

To determine the effect of c-myc-asODNs on metastatic tumor growth in an experimental metastasis model, we injected MZ2-MEL melanoma cells i.v. into nude mice, simulating metastasis. ODNs, free or liposome-entrapped, were injected i.v. at a dose of 2.5 mg/kg once a week over a period of 4 weeks. Only the GD_2-targeted c-*myc* asODN formulation significantly ($P < 0.01$) inhibited the formation and growth of lung metastases (Table 1). There was no statistically significant difference in the tumor growth of mice comparing untreated with those treated with either free or nontargeted asODNs. Moreover, a scrambled sequence containing the G-quartet motif present in myc-as was not efficacious when entrapped in aGD_2-CCL. Histological analysis of lungs stained with the S-100 antibody specific for melanoma cells showed a marked decrease in the metastatic areas in mice treated with aGD_2-CCL-myc-as compared with CCL-myc-as and saline controls (Fig. 4). No sign of treatment-related toxicity, such as inflammation, bleeding, hepatomegaly and splenomegaly, or weight loss to the animals, was observed in the animals over the course of the study.

The effects of aGD_2-CCL-myc-as on human melanoma

Table 1 Inhibition of MZ2-MEL human melanoma lung metastases in nude mice by treatment with GD_2-targeted c-myc-asODN liposomal formulation

	Lung metastases (%)
Control	70–90[a]
Free-myc-as	70–90
CCL-myc-as	60–80
aGD_2-CCL-myc-as	0–10[b]
aGD_2-CCL-myc-scr	70–80

[a] MZ2-MEL human melanoma cells (5×10^6) were injected i.v. in nu/nu mice on day 0. On days 1, 8, 15, and 22, mice received i.v. 2.5 mg/kg c-myc-antisense ODN, free (free-myc-as) or encapsulated in either CCL or anti-GD_2-CCL (CCL-myc-as and aGD_2-CCL-myc-as, respectively). HEPES buffer (pH 7.4) and aGD_2-CCL-myc-scr were also used in mice as control. After 90 days, the lungs were surgically removed from the mice (10 mice/group), fixed in 10% buffered formalin, processed for paraffin embedding, sectioned at 5 μm, and stained with H&E. The experiment was performed twice, and the data represent the percentage of mice presenting lung metastases.

[b] $P < 0.01$ *versus* untreated animals.

tumor growth *in vivo* were also examined using s.c. implanted tumor xenografts in nude mice. In these studies, asODNs, free or liposome encapsulated, were administered i.v. to tumor-bearing mice at 5 days after implantation, at which time tumors were approximately 5 mm in diameter. The tumors grew rapidly in untreated control mice, resulting in the euthanasia of all mice by 4–5 weeks (Fig. 5). In contrast, mice receiving the GD_2-targeted c-*myc* asODN formulation showed a pronounced delay in tumor growth, with a significant ($P < 0.01$ *versus* control mice) increase in life span evaluated as the time it took for the tumors to reach 2000 mm^3 when the mice where euthanized. Moreover, at the end of the observed period (3 months), 2 of 10 mice showed no evidence of tumor and were presumed cured by the treatment. Notably, no other treatment showed any reduction of tumor growth or cured animals.

The antitumor effect for aGD2-CCL-myc-as along with the lack of antitumor activity for the control scrambled sequence (Table 1 and Fig. 5) supports the conclusion that the results observed for immunoliposomal myc-as occur through an antisense mechanism of action.

Inhibition of c-*myc* Protein Expression and Induction of Apoptosis by Immunoliposome-Encapsulated c-myc-asODNs in Tumor Xenografts. To provide evidence that the antitumor activity of aGD_2-CCL-myc-as was caused by its ability to down-regulate *c-myc* protein expression *in vivo*, we analyzed tumor xenografts treated as described previously, by Western blot analysis. Fig. 6*A* shows an immunoblot of whole tumor lysates from representative tumor xenografts. Densitometric analysis of *c-myc* protein expression, normalized to the relative β-actin levels, demonstrated approximately a 75% reduction in c-myc expression on day 4 in tumors from mice treated with aGD_2-CCL-myc-as. In contrast, c-myc protein levels detected in tumors from mice treated with free-myc-as, CCL-myc-as, and aGD_2-CCL-myc-scr were equivalent to levels of untreated tumors.

Melanoma tumors were processed for routine histology and IHC using antibodies specific for melanoma cells (S-100) and for cell proliferation (MIB-1). A major reduction of MIB-1-positive cells in tumors of mice treated with aGD_2-CCL-myc-as was observed (Fig. 6*B*). In contrast, by probing the individual tumor sections with an antibody to CD31, a marker of endothelial cells, we did not observe any difference in blood vessel density among the various treatments (data not shown).

Finally, to determine whether aGD_2-CCL-myc-as induced apoptosis in the tumors, we performed TUNEL staining 1 week after the start of treatment to detect the presence of apoptotic nuclei *in situ*. Only a few isolated TUNEL-positive nuclei were visible in untreated tumors and those treated with CCL-myc-as. In contrast, tumors treated with aGD_2-CCL-myc-as clearly showed high levels of apoptotic nuclei (Fig. 6*B*). Thus, c-*myc* asODNs entrapped in aGD_2 immunoliposomes reduced c-myc protein levels and induced apoptosis in the tumor xenografts.

Induction of *p53* and Inhibition of *Bcl-2* Protein Expression by Immunoliposome-Encapsulated c-myc-asODNs *in Vivo*. "Intrinsic stresses," such as oncoproteins (*e.g.*, c-*myc*), can activate the intrinsic apoptotic pathway. As a sensor of cellular stress, *p53* is a critical initiator of this pathway by transcriptionally repressing antiapoptotic Bcl-2 proteins (6, 7). To examine the role of *p53* and *Bcl-2* in the response of melanoma cells to targeted liposomal c-*myc* antisense, *p53* and *Bcl-2* protein expressions were examined in the tumor xenografts (Fig. 6*B*). Control melanoma tumors did not exhibit almost any immunostaining for p53 (<5% positive cells), while showing a strong positivity for Bcl-2 (>75%). In contrast, only tumors treated with aGD_2-CCL-myc-as clearly showed enhanced p53 immunoreactivity (>75%) and drastic reduction of Bcl-2 protein staining (<5%).

To further pursue mechanisms of apoptosis induced by aGD_2-CCL-myc-as in melanoma xenografts, we investigated the kinetic of changes in c-myc, p53, and Bcl-2 expression on Western blot (Fig. 7). Densitometric analysis of c-myc protein expression, normalized to the relative β-actin levels, demonstrated a time-dependent reduction in its expression starting already after 24 h of treatment (about 25%) and reaching approximately 80% after 96 h. Treatment with aGD_2-CCL-myc-as caused an induction in the expression of p53 protein after 48 h, which was more marked at longer times. Induction of p53 by aGD_2-CCL-myc-as was associated with a delayed decrease of expression of the antiapoptotic protein Bcl-2 (48–72 h after treatment, 10–30% reduction). At the last time point observed, Bcl-2 protein was reduced by approximately 75% of the control melanoma cells level.

DISCUSSION

We have shown that an asODN complementary to the translation region of c-*myc* mRNA inhibited the growth of melanoma cells *in vitro* and *in vivo* and that its inhibitory effect was greatest when it was delivered to the cells via sterically stabilized liposomes targeted against the GD_2 epitope expressed at the cell surface. The c-*myc* proto-oncogene plays a key role in cell proliferation, differentiation, and apoptosis (4). By using anti-GD_2-targeted liposomal formulations of c-myc-asODNs, we have clearly demonstrated that the down-modulation of c-*myc* reduced cell proliferation and tumorigenicity and increased the apoptotic rate of human melanoma. The mechanism for the antiproliferative effect appears to be down-regulation of

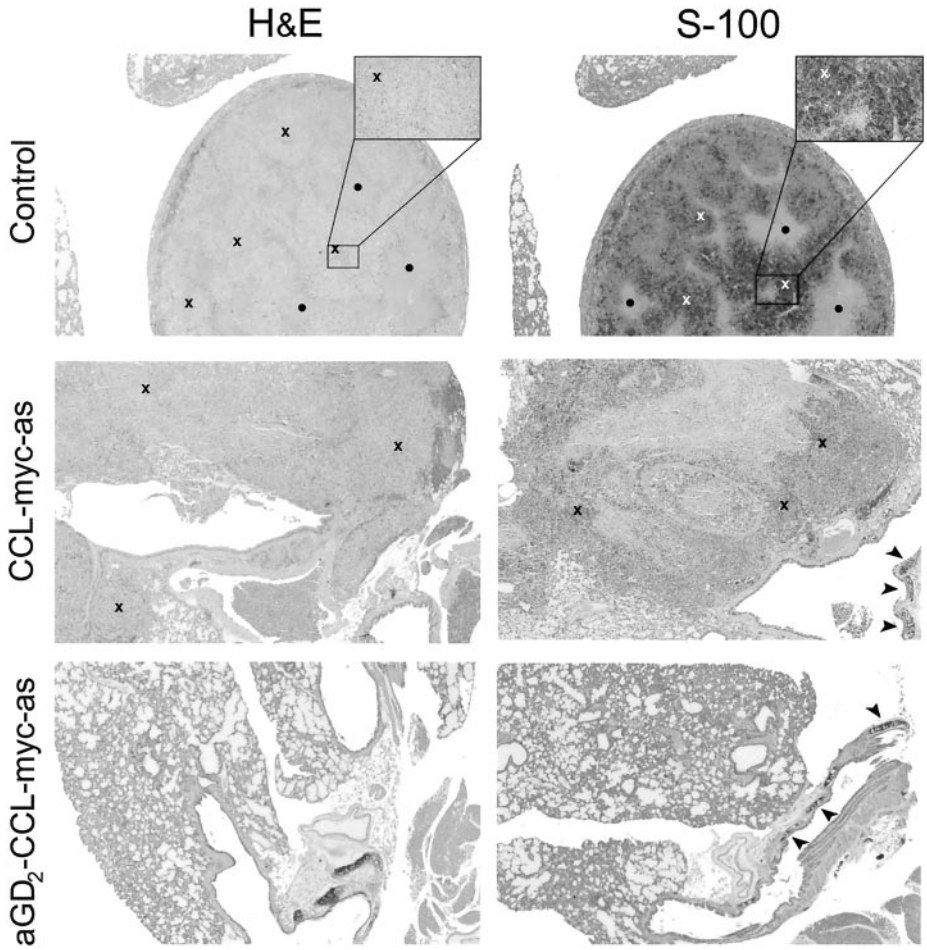

Fig. 4 Histology (H&E) analysis and IHC staining for S-100 protein. Nude mice received i.v. injections of MZ2-MEL cells and were treated following the schedule reported in Table 1. After 120 days, the lungs were surgically removed from the mice, fixed in 10% buffered formalin, processed for paraffin embedding, sectioned at 5 μm, and stained with both H&E and S-100. Metastatic tumor infiltration (*x*) and necrotic area (●) in the lungs of untreated mice or those treated with nontargeted CCL-myc-as are shown compared with mice treated with aGD_2-CCL-myc-as, which did not present any pulmonary metastatic localization. *Arrowhead*, internal positive control of IHC staining for S-100 protein, which is physiologically expressed by pulmonary chondrocytes. Magnitude, ×4 (*inset*, ×40).

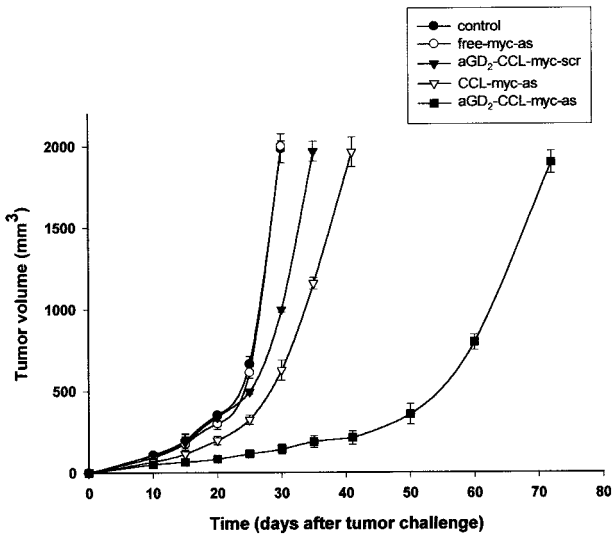

Fig. 5 Therapeutic efficacy of GD_2-targeted c-myc-asODN liposomal formulation in MZ2-MEL melanoma-bearing mice. All nude mice received treatments (i.v.) on day 5 after s.c. injection of 5×10^6 MZ2-MEL: 3.5 mg ODN per kilogram of mouse weight, every day for 3 days; HEPES buffer (pH 7.4) was used as control.

the expression of the c-myc proliferative protein by these tumors and interruption of c-*myc*-mediated signaling: activation of *p53* and down-modulation of the antiapoptotic protein Bcl-2. This, in turn, leads to extensive tumor apoptosis resulting in significant growth arrest of the tumors. These findings, together with the results of previous investigations that demonstrated growth inhibition of malignant melanoma cells caused by the addition of asODNs targeted to c-*myc* mRNA (15, 22), suggest that this key mediator of cell proliferation and apoptosis has a crucial function(s) in the development of this malignancy.

Human neuroectoderma-derived tissues can undergo malignant transformation both in adulthood and in the pediatric population, giving rise to tumors among which small cell lung cancer, melanoma, and neuroblastoma are the most frequent. Moreover, although the overall cancer incidence has been declining by 0.7% annually in recent years, melanoma and tumors of the lymphoid system are rising at a rate of about 2.5% a year (1, 2). Overall, patients suffering from malignant melanoma often present with advanced disease and have a poor prognosis. Despite aggressive therapeutic protocols, the overall long-term disease-free survival rate has not been significantly prolonged (34). Recently, several new strategies have emerged to circumvent this unfavorable scenario.

The strategy of down-regulating cell proliferation through

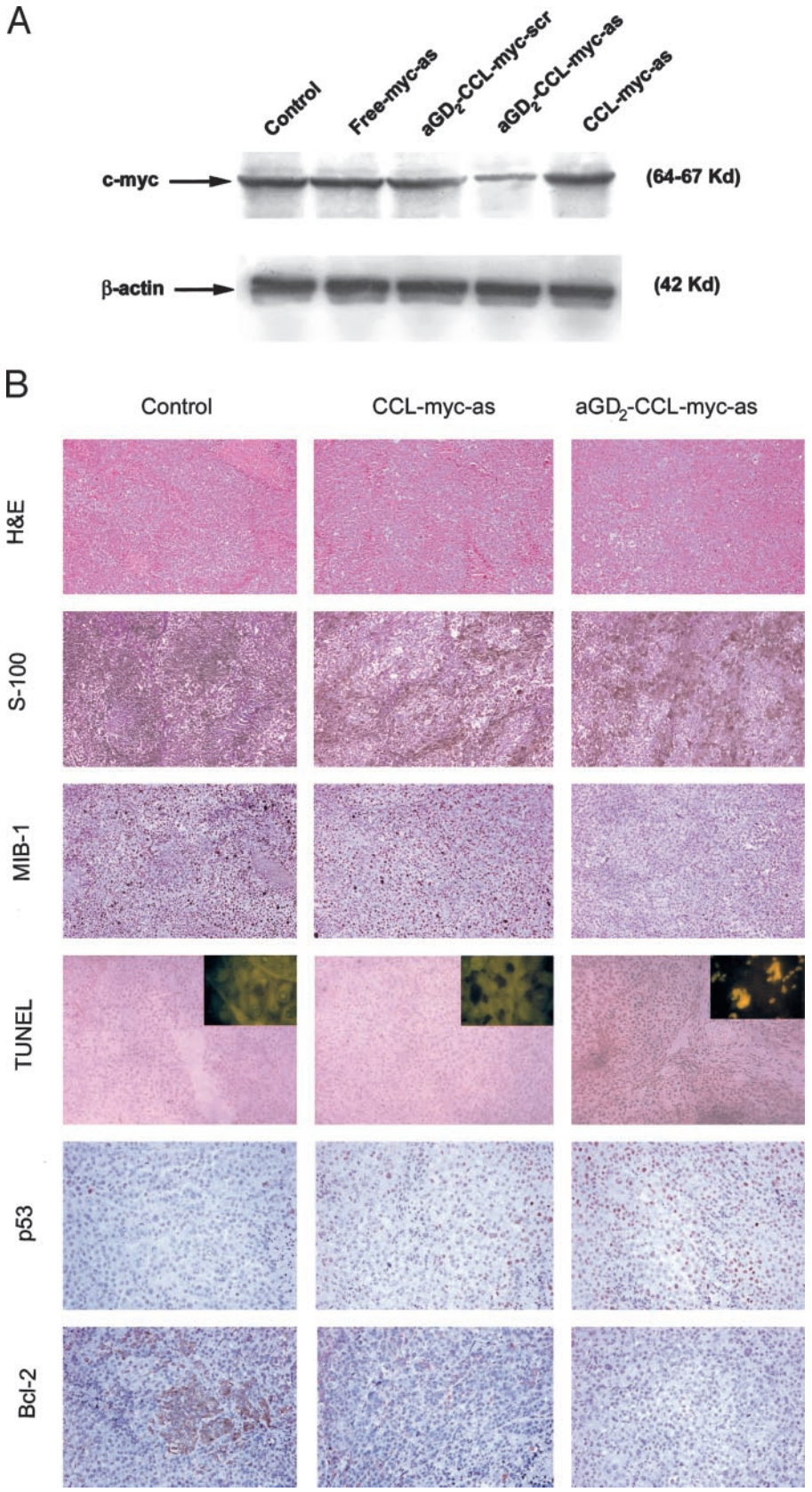

Fig. 6 Inhibition of target protein expression and induction of apoptosis in tumor xenografts. Nude mice received s.c. injections of MZ2-MEL cells and were treated as reported in the legend to Fig. 4. *A*, immunoblotting of tumor lysates was performed as described in "Materials and Methods" to quantify the level of c-myc in control mice or mice treated with free antisense or aGD_2-CCL-myc-as or aGD_2-CCL-myc-scr. Analysis was performed at day 4 after the end of treatment. Bands from one representative tumor per group are shown. *B*, IHC analysis. One week after the end of treatment, primary tumors were harvested and processed as described in the legend to Fig. 4. Tissue sections were also immunostained for expression of MIB-1, to show proliferation; for TUNEL (*inset*, FITC), to show apoptosis; and for p53 and Bcl-2, to detect apoptotic regulatory proteins. Original magnification: H&E, S-100, MIB-1, and TUNEL, ×10 (*inset*, ×100); p53 and Bcl-2, ×20.

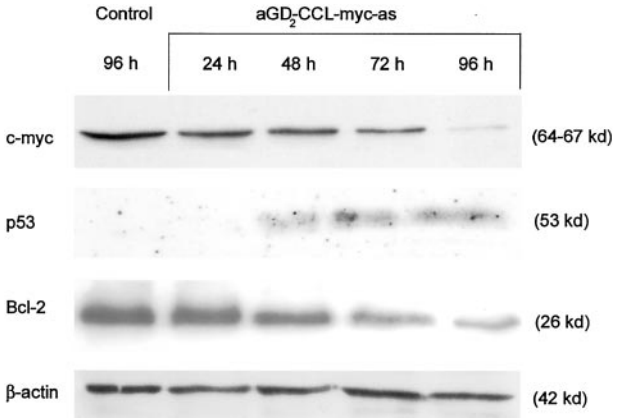

Fig. 7 Western blot analysis of c-myc, p53, Bcl-2, and β-actin protein levels as a function of time of treatment with aGD_2-CCL-myc-as. As described in "Materials and Methods," immunoblotting of tumor lysates was performed at 24-h intervals after terminating treatment of the s.c. tumors to quantify the level of c-myc, p53, Bcl-2, and β-actin protein in control mice or mice treated with aGD_2-CCL-myc-as. Bands from one representative tumor per group are shown.

inhibition of proliferative gene products with asODNs is a compelling one. AsODNs take direct advantage of molecular complementarity (35, 36) to inhibit gene expression in a sequence-specific manner. This conceptually simple, straightforward, and rational approach to novel drug design is attractive for the treatment of cancers and other human diseases (9–12, 36). However, realizing the therapeutic potential of asODN is more complicated, for several reasons. These include the need to deliver asODNs selectively to diseased tissues to maximize their action and to minimize their side effect, instability of the asODNs *in vivo* and their unfavorable pharmacokinetics, and the lack of transfer of the asODNs across cell membranes. A recently developed therapeutic strategy that addresses many of these potential problems uses liposomes as carriers for asODNs (18, 21, 22, 29).

Here, we have described a system in which asODNs are encapsulated within small, long-circulating, target-specific liposomes directed against the internalizing GD_2 epitope, which is extensively expressed on melanoma cells relative to normal tissues in the peripheral nervous system and the cerebellum (27). The liposomes have trapping efficiencies of 90% or greater for the asODNs. Applications of asODNs *in vivo* could benefit from the use of long-circulating, targeted liposomal carriers for several reasons: (*a*) entrapment within liposomes could increase the distribution of asODNs to target tissues and away from sites of metabolism and excretion (21); (*b*) liposome entrapment will retard loss of the antisense through the kidneys and avoid rapid degradation by extracellular nucleases; (*c*) the protection provided by the liposomal formulations may obviate the need for unnatural backbone chemistries; and (*d*) as a result of their large carrying capacity, targeted liposomes can deliver large numbers of asODN molecules for each binding event. The ability of liposome entrapment to substantially decrease the clearance of the asODN undoubtedly contributed to their ability to inhibit tumor metastases and delay tumor growth, which we observed at low doses of aGD_2-CCL-myc-as (Fig. 3). These data are in agreement with previous findings demonstrating a strong correlation between antitumor activity and circulation longevity of liposome-entrapped drugs in different animal models (22, 37).

It is notable that significant inhibition of experimental metastases and s.c. tumor growth occurred at i.v. doses of asODN of only 2.5 mg/kg weekly × 4 or 3.5 mg/kg every 2 days × 3, respectively. These are very low levels of asODN compared with the amounts of free asODN or other nontargeted liposomal preparations required for activity *in vivo* (9–15, 22, 38). Thus, important factors contribution to these results might be (*a*) the specific binding and receptor-mediated internalization of our formulation into the target cells and (*b*) the long circulation times that allow a greater portion of our formulation to reach the target cells.

One of the most attractive features of antisense-based antiproliferative therapeutics is their potential for a high degree of specificity (8). However, antisense effects can also be caused by sequence-specific interactions between ODNs and cellular proteins that can cause the so-called "sequence-dependent, nonantisense effect." For example, the presence of four contiguous guanosine residues in an ODN (the G quartet) and/or the CpG motifs, can result in immune stimulation leading to an antiproliferative effect that is not an antisense effect *per se* (16, 39). Because the scrambled sequence herein used also contains both the G quartet and the CpG regions, these additional mechanisms underlying its action can be ruled out in our model.

The evidence from human tumors that cancer generally requires impaired apoptosis is not yet overwhelming, but the hypothesis is strongly supported by experimental models. In particular, the oncogenic potential of elevated Bcl-2 has been clearly shown in several transgenic mouse models (7). *Myc*-aided transformation of Bcl-2-expressing cells and coexpression of *Bcl-2* and *myc* transgenes dramatically accelerated lymphomagenesis (5, 7). Given that many of the apoptotic regulators altered in resistant tumors have been identified (6), one new approach to therapy is to restore apoptotic potential through genetic or pharmacological methods. The direct relationship between *p53*, apoptosis, and drug action implies that restoring *p53* activity in *p53* null tumors, or activating apoptotic pathways that are directly downstream of *p53*, would have clinical benefits. Moreover, mutations in *TP53* (the gene that encodes p53) are common in some cancers and lead to resistance to DNA-damaging agents. *TP53* mutations are not common in melanoma, but the *p53* pathway might be impaired by mutations in the *p53* activation pathway (40). In this regard, the prospect of directly switching on the apoptotic machinery *in vivo* into melanoma cells by activating the "classical" intrinsing mitochondrial pathway to apoptosis, regulated by the interplay of c-*myc*, *p53*, and *Bcl-2* and resulting in the activation of the caspase cascade (41), would be of great clinical interest.

Despite the positive outlook for antisense inhibitors targeted against c-*myc* for the treatment of melanoma, some potential limitation may exist for this approach. For example, little is known about the potential for development of resistant tumor cell populations that lose their sensitivity toward c-*myc* inhibition over time. Because some degree of resistance in target cells occurs for virtually all chemotherapeutic drugs in the clinical setting, resistance to antisense may also develop. On the positive side, our results suggest that encapsulation of asODNs in GD_2-

targeted liposomes can protect nontargeted cells from potential deleterious effects of the asODNs, while simultaneously enhancing the toxicity of the molecule toward the target cell population. However, one cannot expect that even the most target-specific liposomes will affect only the target cell population. A portion of the dose could accumulate in other tissues with potentially toxic consequences.

The advantages of liposome-encapsulated chemotherapeutics over free molecules have been demonstrated in several animal models of cancer (42, 43), mainly against small primary and micrometastatic solid tumors (25, 30, 44). As a note of caution, immunoliposomes appear to lose their advantage when attempts are made to treat established advanced solid tumors (43, 44), likely because the "binding site barrier" restricts penetration of SIL into the tumor (45). The role of adjuvant therapy in the treatment of patients with intermediate risk and high-risk malignant melanoma remains an area of intense investigation (46, 47), and although several trials are currently ongoing (48), vaccine therapy has failed to clearly demonstrate a survival benefit. Thus, the use of myc-as, encapsulated into GD_2-targeted liposomes, may hold promise as adjuvant therapy for the treatment of human melanoma or for disease resulting from incomplete surgery or early micrometastatic lesions.

ACKNOWLEDGMENTS

The mAb 14.G2a, a murine mAb of IgG2a isotype subclass, specific for the GD_2 antigen, was kindly provided by R. A. Reisfeld (The Scripps Institute, La Jolla, CA). We thank Prof. G. Zupi for kindly providing us with human melanoma cell lines; E. Moase, F. Salutari, and L. Tedeschi for expert technical assistance; and Drs. P. G. Montaldo, M. V. Corrias, and V. Pistoia for helpful discussions.

REFERENCES

1. Balch, M., Houghton, A., and Peters, L. Cutaneous Melanoma. *In:* V. T. DeVita, Jr., S. Hellman, and S. A. Rosenberg (eds.), Cancer Principles of Oncology, pp. 1499–1542. Philadelphia: Lippincott-Raven, 1989.

2. Marshall, E. Cancer warriors claim a victory. Science (Wash. DC), *279:* 1842–1843, 1998.

3. Cole, M. D. The myc oncogene: its role in transformation and differentiation. Annu. Rev. Genet., *20:* 361–384, 1986.

4. Dang, C. V. c-Myc target genes involved in cell growth, apoptosis, and metabolism. Mol. Cell. Biol., *19:* 1–11, 1999.

5. Green, D. R., and Evan, G. I. A matter of life and death. Cancer Cell, *1:* 19–30, 2002.

6. Johnstone, R. W., Ruefli, A. A., and Lowe, S. W. Apoptosis: a link between cancer genetics and chemotherapy. Cell, *108:* 153–164, 2002.

7. Cory, S., and Adams, J. M. The Bcl2 family: regulators of the cellular life-or-death switch. Nat. Rev. Cancer, *2:* 647–656, 2002.

8. Crooke, S. T. Therapeutic applications of oligonucleotides. Annu. Rev. Pharmacol. Toxicol., *32:* 329–376, 1993.

9. Monia, B. P., Johnston, F. J., Geiger, T., Muller, M., and Fabbro, D. Antitumor activity of a phosphorotioate antisense oligodeoxynucleotide targeted against C-raf kinase. Nat. Med., *2:* 668–675, 1996.

10. Neurath, M. F., Pettersson, S., Meyer zum Buchenfelde, K. H., and Strober, W. Local administration of antisense phosphoothioate oligonucleotides to the p65 subunit of NF-kB abrogates established experimental colitis in mice. Nat. Med., *2:* 998–1004, 1996.

11. Heere-Ress, E., Thallinger, C., Lucas, T., Schlagbauer-Wadl, H., Wacheck, V., Monia, B. P., Wolff, K., Pehamberger, H., and Jansen, B. Bcl-X(L) is a chemoresistance factor in human melanoma cells that can be inhibited by antisense therapy. Int. J. Cancer, *99:* 29–34, 2002.

12. Eberle, J., Fecker, L. F., Bittner, J. U., Orfanos, C. E., and Geilen, C. C. Decreased proliferation of human melanoma cell lines caused by antisense RNA against translation factor eLF-4A1. Br. J. Cancer, *86:* 1957–1962, 2002.

13. Skorski, T., Perrotti, D., Nieborowska-Skorski, M., Gryaznov, S., and Calabretta, B. Antileukemia effect of c-myc N3′-P5′ phosphoramidate antisense oligonucleotides in vivo. Proc. Natl. Acad. Sci. USA, *94:* 3966–3971, 1997.

14. Citro, G., D'Agnano, I., Leonetti, C., Perini, R., Bucci, B., Zon, G., Calabretta, B., and Zupi, G. c-myc antisense oligodeoxynucleotides enhance the efficacy of cisplatin in melanoma chemotherapy in vitro and in nude mice. Cancer Res., *58:* 283–289, 1998.

15. Leonetti, C., D'Agnano, I., Lozupone, F., Valentini, A., Geiser, T., Zon, G., Calabretta, B., Citro, G., and Zupi, G. Antitumor effect of c-myc antisense phosphorothioate oligodeoxynucleotides on human melanoma cells in vitro and in mice. J. Natl. Cancer Inst., *88:* 419–429, 1996.

16. Wagner, R. W. The state of the art in antisense research. Nat. Med., *1:* 1116–1118, 1995.

17. Wang, S., Lee, R. J., Cauchon, G., Gorestein, D. G., and Low, P. S. Delivery of antisense oligodeoxyribonucleotides against the human epidermal growth factor receptor into cultured KB cells with liposomes conjugated to folate via polyethylene glycol. Proc. Natl. Acad. Sci. USA, *92:* 3318–3322, 1995.

18. Zelphati, O., and Szoka, F. C. J. Liposomes as a carrier for intracellular delivery of antisense oligonucleotides: a real or magic bullet? J. Control. Rel., *41:* 99–119, 1996.

19. Gokhale, P. C., Soldatenkov, V., Wang, F. H., Rahman, A., Dritschilo, A., and Kasid, U. Antisense raf oligodeoxynucleotide is protected by liposomal encapsulation and inhibits Raf-1 protein expression in vitro and in vivo: implications for gene therapy of radioresistant cancer. Gene Ther., *4:* 1289–1299, 1997.

20. Guterriez-Puente, Y., Tari, A. M., Stephens, C., Rosenblum, M., Guerra, R. T., and Lopez-Berestein, G. Safety, pharmacokinetics, and tissue distribution of liposomal P-ethoxy antisense oligonucleotides targeted to Bcl-2. Pharmacol. Exp. Ther., *291:* 865–869, 1999.

21. Stuart, D. D., Kao, G. Y., and Allen, T. M. A novel, long-circulating, and functional liposomal formulation of antisense oligodeoxynucleotides targeted against MDR1. Cancer Gene Ther., *7:* 466–475, 2000.

22. Leonetti, C., Biroccio, A., Benassi, B., Stringaro, A., Stoppacciaro, A., Semple, S. C., and Zupi, G. Encapsulation of c-myc antisense oligodeoxynucleotides in lipid particles improves antitumoral efficacy in vivo in a human melanoma line. Cancer Gene Ther., *8:* 459–468, 2001.

23. Allen, T. M., and Moase, E. H. Therapeutic opportunities for targeted liposomal drug delivery. Adv. Drug Del. Rev., *21:* 117–133, 1996.

24. Pagnan, G., Montaldo, P. G., Pastorino, F., Raffaghello, L., Kirchmeier, M., and Allen, T. M. GD2-mediated melanoma cell targeting and cytotoxicity of liposome-entrapped fenretinide. Int. J. Cancer, *81:* 268–274, 1999.

25. Pastorino, F., Brignole, C., Marimpietri, D., Sapra, P., Moase, E. H., Allen, T. M., and Ponzoni, M. Doxorubicin-loaded Fab′ fragments of anti-disialoganglioside immunoliposomes selectively inhibit the growth and dissemination of human neuroblastoma in nude mice. Cancer Res., *63:* 86–92, 2003.

26. Raffaghello, L., Pagnan, G., Pastorino, F., Cosimo, E., Brignole, C., Marimpietri, D., Montaldo, P. G., Gambini, C., Allen, T. M., Bogenmann, E., and Ponzoni, M. In vitro and in vivo antitumor activity of liposomal Fenretinide targeted to human neuroblastoma. Int. J. Cancer, *104:* 559–567, 2003.

27. Schulz, G., Cheresh, D. A., Vark, N. M., Yu, A., Staffileno, L. K., and Reisfeld, R. A. Detection of ganglioside GD2 in tumor tissues and sera of neuroblastoma patients. Cancer Res., *44:* 5914–5920, 1984.

28. Pagnan, G., Stuart, D. D., Pastorino, F., Raffaghello, L., Montaldo, P. G., Allen, T. M., Calabretta, B., and Ponzoni, M. Delivery of c-myb antisense oligodeoxynucleotides to human neuroblastoma cells via di-

sialoganglioside GD2-targeted immunoliposomes: antitumor effects. J. Natl. Cancer Inst., *92:* 253–261, 2000.

29. Stuart, D. D., and Allen, T. M. A new liposomal formulation for antisense oligodeoxynucleotides with small size, high incorporation efficiency and good stability. Biochim. Biophys. Acta, *1463:* 219–229, 2000.

30. Kirpotin, D., Park, J. W., Hong, K., Zalipsky, S., Li, W. L., Carter, P., Benz, C. C., and Papahadjopoulos, D. Sterically stabilized anti-HER2 immunoliposomes: design and targeting to human breast cancer cells *in vitro*. Biochemistry, *36:* 66–75, 1997.

31. Pastorino, F., Stuart, D. D., Ponzoni, M., and Allen, T. M. Targeted delivery of antisense oligonucleotides in cancer. J. Control. Rel., *74:* 69–75, 2001.

32. Ribatti, D., Polimeno, G., Vacca, A., Marzullo, A., Crivellato, E., Nico, B., Lucarelli, G., and Dammacco, F. Correlation of bone marrow angiogenesis and mast cells with tryptase activity in myelodysplastic syndromes. Leukemia (Baltimore), *16:* 1680–1684, 2002.

33. Allen, T. M., and Hansen, C. Pharmacokinetics of stealth versus conventional liposomes: effect and dose. Biochim. Biophys. Acta, *1068:* 133–141, 1991.

34. Middleton, M. R., Lorigan, P., and Owen, J. A randomized phase III study comparing decarbazine, BCNU, cisplatin and tamoxifen with decarbazine and interferon in advanced melanoma. Br. J. Cancer, *82:* 1158–1162, 2000.

35. Stein, C., and Cheng, Y. C. Antisense oligonucleotides as therapeutic agents. Is the bullet really magical? Science (Wash. DC), *261:* 1004–1012, 1993.

36. Galderisi, U., Cascino, A., and Giordano, A. Antisense oligonucleotides as therapeutic agents. J. Cell. Physiol., *181:* 251–257, 1999.

37. Webb, M. S., Harasym, T. O., Masin, D., Bally, M. B., and Mayer, L. D. Sphingomyelin-cholesterol liposomes significantly enhance the pharmacokinetic and therapeutic properties of vincristine in murine and human tumor models. Br. J. Cancer, *72:* 896–904, 1995.

38. Smith, J. B., and Wickstrom, E. Antisense c-myc and immunostimulatory oligonucleotide inhibition of tumorigenesis in a murine B-cell lymphoma transplant model. J. Natl. Cancer Inst., *90:* 1146–1154, 1998.

39. Tamm, I., Dorken, B., and Hartmann, G. Antisense therapy in oncology: new hope for an old idea?. Lancet, *358:* 489–497, 2001.

40. Hersey, P., and Zhang, X. D. How melanoma cells evade trail-induced apoptosis. Nat. Rev. Cancer, *1:* 142–150, 2001.

41. Shi, Y. Mechanisms of caspase activation and inhibition during apoptosis. Mol. Cell, *9:* 459–470, 2002.

42. Huwyler, J., Wu, D., and Pardridge, W. M. Brain drug delivery of small molecules using immunoliposomes. Proc. Natl. Acad. Sci. USA, *93:* 14164–14169, 1996.

43. Lopez De Menezes, D. E., Pilarski, L. M., and Allen, T. M. *In vitro* and *in vivo* targeting of immunoliposomal doxorubicin to human B-cell lymphoma. Cancer Res., *58:* 3320–3330, 1998.

44. Allen, T. M., Ahmad, I., Lopez De Menezes, D. E., and Moase, E. H. Immunoliposome mediated targeting of anti-cancer drugs *in vivo*. Biochem. Soc. Trans., *23:* 1073–1079, 1995.

45. Yuan, F., Leunig, M., Huang, S. K., Berk, D. A., Papahadjopoulos, D., and Jain, R. K. Microvascular permeability and interstitial penetration of sterically stabilized (stealth) liposomes in a human tumor xenograft. Cancer Res., *54:* 3352–3356, 1994.

46. McClay, E. F. Adjuvant therapy for patients with high-risk malignant melanoma. Semin. Oncol., *29:* 389–399, 2002.

47. Eggermont, A. M., and Gore, M. European approach to adjuvant treatment of intermediate- and high-risk malignant melanoma. Semin. Oncol., *29:* 382–388, 2002.

48. DiFronzo, L. A., Gupta, R. K., Essner, R., Foshag, L. J., O'Day, S. J., Wanek, L. A., Stern, S. L., and Morton, D. L. Enhanced humoral immune response correlates with improved disease-free and overall survival in American Joint Committee on Cancer stage II melanoma patients receiving adjuvant polyvalent vaccine. J. Clin. Oncol., *20:* 3242–3248, 2002.

Clinical Cancer Research

Targeted Liposomal c-*myc* Antisense Oligodeoxynucleotides Induce Apoptosis and Inhibit Tumor Growth and Metastases in Human Melanoma Models

Fabio Pastorino, Chiara Brignole, Danilo Marimpietri, et al.

Clin Cancer Res 2003;9:4595-4605.